Effect of Conformational Symmetry upon the Formation of Cysteine Clusters on the Au(110)−(1 × 1) Surface: A First−Principles Study

ARTICLE *in* THE JOURNAL OF PHYSICAL CHEMISTRY C · SEPTEMBER 2013

Impact Factor: 4.77 · DOI: 10.1021/jp4072857

2 AUTHORS:

Luiza Buimaga-Iarinca
National Institute for Research and Developm…
21 PUBLICATIONS **56** CITATIONS
SEE PROFILE

Cristian Morari
National Institute for Research and Developm…
41 PUBLICATIONS **203** CITATIONS
SEE PROFILE

THE JOURNAL OF PHYSICAL CHEMISTRY C

Article

pubs.acs.org/JPCC

Effect of Conformational Symmetry upon the Formation of Cysteine Clusters on the Au(110)-(1 × 1) Surface: A First-Principles Study

Luiza Buimaga-Iarinca and Cristian Morari*

National Institute for Research and Development of Isotopic and Molecular Technologies, 65-103 Donath Street, 400293 Cluj-Napoca, Romania

ABSTRACT: The physical properties of cysteine clusters formed on the Au(110)-(1 × 1) surface are investigated by means of density-functional theory. We take into account the clusters formed from three types of rotational conformers of cysteine; for each structure we investigate the protonated and unprotonated forms. Our investigations are based on three different geometrical models for the surface−adsorbate system, allowing us to describe the formation of new nucleation centers on the surface as well as the properties of long chains of cysteine molecules adsorbed on the Au(110)-(1 × 1) surface. We point out significant differences between the relaxed structures formed by each conformer as well as the specific physicochemical properties leading to formation of new nucleation centers compared with those of already formed large cysteine structures. In particular, we emphasize the role of the NH_2 group of cysteine in these processes, by correlating our data with its relative position with respect to the gold surface.

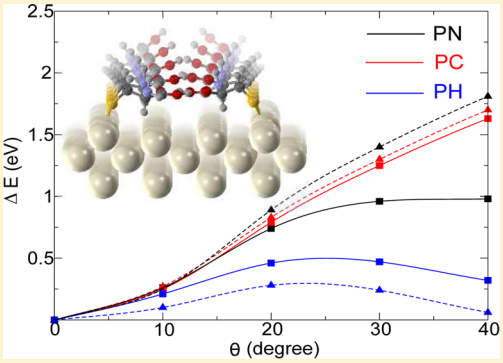

INTRODUCTION

The adsorption of organic molecules on noble metal surfaces has attracted much scientific interest in recent years. An increasing number of organic molecules were prepared in the past decade with the objective of building self-assembled monolayer (SAM) structures functionalized on various surfaces.[1−4] The increasing interest in the physical properties of metal−organic interfaces is reflected in the wide range of structures studied in this context.[5−10] They go from small molecular structures[11−15] to DNA or its components.[16−18]

The amino acid cysteine ($HS\text{-}CH_2\text{-}CH(NH)_2\text{-}COOH$) is one of the most interesting examples for the adsorption of biomolecules holding a real potential for the practical applications in the functionalization of surfaces. Experimental studies revealed interesting phenomena, such as the formation of homochirally adsorbed dimers,[19] unidirectional molecular rows,[20,21] and large homochiral molecular islands growing from chiral kink sites[20]—all occurring in the Au(110)-(1 × 2) surfaces. For the missing-row reconstructed Au(110)-(1 × 2) surface the formation of the cysteine clusters of small size was evidenced by Kühnle at al.[21] They argued that the molecular configuration of the clusters is such that it allows all molecular interaction points to be saturated by specific interactions to other molecules within the cluster or to surface atoms, preventing the attachment of additional molecules. Also, it was assumed that the clusters evidenced by scanning tunneling microscopy (STM) probably consist of a single layer of protonated cysteine molecules. These results suggested that cysteine molecules self-assemble on the Au(110) surface not because of significant intermolecular interactions along the row direction but because the molecules preferentially adsorb in unidirectional trenches created by the removal of atoms from the close-packed gold rows of the missing rows in the Au(110)-(1 × 2) surface.[20] It was also argued that the formation of extended molecular rows, as opposed to individually adsorbed or clustered molecules, minimizes the energy cost associated with this surface rearrangement, providing an effective intermolecular attraction which acts as the driving force for the molecular self-assembly process.

The properties of chiral recognition by atomic kinks were emphasized by the studies performed on the Au(17 11 9) surface.[22,23] These findings were supported by DFT calculations of Šljivančanin et al.[24]

On the theoretical side several studies were concerned with elucidation of the details of cysteine−gold interaction[25−28] as well as the study of enantiomeric adsorption on chiral surfaces.[24] Höffling et al.[27] found that flat adsorption configurations with S−Au at an off-bridge site and NH_2−Au at an off-top site are energetically favored in the adsorption process on the Au(110) surface. Also, sulfur−substrate interaction via an unprotonated thiolate group has been shown to create stronger bonds than dimer disulfide bonding on Au(111).[26] Höffling et al.[27] pointed out that the binding energy of the thiolate bond is very sensitive to the changes of the bonding geometry. Also, they found out that the formation of the thiolate bond does not lead to a charge transfer between the molecule and the surface. On the other hand, the interaction between NH_2 and gold leads to an important charge transfer between the molecule and surface (about 0.6−0.7 *e*). It was concluded that the molecule prefers a flat

Received: July 23, 2013
Revised: September 6, 2013
Published: September 6, 2013

   dx.doi.org/10.1021/jp4072857 | *J. Phys. Chem. C* 2013, 117, 20351−20360

adsorption geometry, allowing for the formation of an additional bond between the molecule and surface, while the tetrahedron-like geometry of the thiolate bond is preserved.

Because of the flexibility of the thiol side chain, cysteine exhibits 71 unique conformers, eleven of them within 0.1 eV of the lowest minimum of the total energy.[29] This value is relatively close to the thermal energy at room temperature (i.e., ≈0.03 eV), suggesting that several different cysteine conformers are used in the experiments, even at room temperature. The differences between the molecule−surface interaction mechanisms determined by the orientation of the NH_2, COOH, and S atoms with respect to the surface[30] point out the necessity for a comparative study of adsorption for selected rotational conformers of cysteine. We choose to investigate adsorption of small clusters formed by three conformers of cysteine. The Newman projections of the structures are indicated in Figure 1,

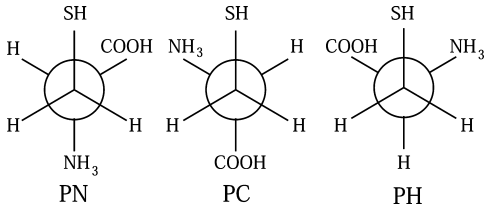

Figure 1. Newman projection for the PN, PC, and PH rotamers of cysteine.

together with their labels: PN, PC, and PH. These geometrical structures allow different functional groups (i.e., carboxylate, thiol, and amino) to interact with the metal surface. Our motivation for the present study is 2-fold: (i) to point out the mechanism of formation of molecular clusters on the Au(110)-(1 × 1) clean surface and (ii) to investigate the specific features for each of the three conformers mentioned above.

COMPUTATIONAL DETAILS

We have calculated the electronic and structural properties of free and adsorbed cysteine clusters within the density functional theory. All calculations were performed using the Siesta code[31,32] that uses norm-conserving pseudopotentials in their fully nonlocal form[33] and expands the wave functions of valence electrons by a linear combinations of atomic orbitals (LCAO). The LCAO basis set used by Siesta[31,32] is defined for minimal (single-ζ) orbitals using the efficient method of Sankey and Niklewski.[34] Precisely, the orbitals are the eigenfunctions of the (pseudo-) atom confined within a spherical box (although the radius of the box may be different for each orbital). In other words, they are the numerical eigenfunctions of the atomic pseudopotential, for an energy $\varepsilon_l + \delta\varepsilon_l$ chosen so that the first node occurs at the desired cutoff radius r_l^c, where $l = 0, 1, 2, \ldots$ is the angular-momentum quantum number for the orbitals s, p, d, ... To obtain a well-balanced basis, in which the effect of the confinement is similar for all the orbitals, a common energy shift $\delta\varepsilon_l$ is defined for all orbitals, rather than a common radius r^c (i.e., the orbital radii depend on the atomic species and angular momentum).

Next, the multiple-ζ orbitals are built using the split-valence method, which is standard in quantum chemistry.[35] The first-ζ basis orbitals are contracted (i.e., fixed) linear combinations of Gaussians, determined either variationally or by fitting numerical atomic eigenfunctions. The second-ζ orbital is then one of the Gaussians (generally the slowest-decaying one), which is split from the contracted combination.

For each conformer we study three types of adsorbed clusters: isolated structures formed by 2 and 4 cysteine units, on one hand, and a periodic model for the cysteine rows formed along the $[1\bar{1}0]$ direction (i.e., 2 cysteine units and periodic boundary conditions). These three models correspond to the formation of new nucleation centers for the growth of self-assembled cysteine structures (the dimer and double dimer) versus long rows of self-assembled cysteine (periodic structure). For all geometric models we study the adsorption of both protonated and unprotonated configurations.

We confined the systems to a unit cells that would naturally allow the study of periodicity of the Au(110)-(1 × 1) surface. The supercell used has a size of 6 × 6 unit cells of the Au(110) surface and 4 layers of atoms, for isolated clusters. For periodic structures we used a 2 × 6 unit cell in the *XOY* plane and 4 layers of gold atoms in the surface. The length of the cell along the *OZ* axis was set to L_Z = 30 Å for all models. A double-ζ polarized basis set with an energy cutoff of 25 meV has been employed; a single k-point was used to model the periodicity along the *Z* axis, while for the transversal direction we use a 2 × 2 grid for isolated clusters. Finally, for periodic systems we use a 4 × 2 k-points grid. The adsorbed molecules were investigated by the generalized gradient approximation (GGA)[36] to the exchange and correlation functional, in the improved version of the PBE functional of Hammer, Hansen, and Nørskov (RPBE).[37]

To build the geometric structures of the clusters we follow the experimental evidence of the formation of unidirectional molecular rows.[20] Also, we take into account the fact that the sulfur is expected to interact with the gold atoms. We built the preliminary geometrical models for the adsorption of PN, PC, and PH cysteine clusters by allowing the S atom of each cysteine to take a position close to the ideal one reported by Höffling et al.[27] Precisely, we chose a configuration with the S atom close to the off-bridge position. An interesting feature to note here is that the adsorption of a single molecule favors the flat orientation with S−Au at an off-bridge site and NH_2−Au at an off-top site.[27] In the case of cluster adsorption the off-bridge position of S may lead to a position that is not convenient for the NH_2 group (i.e., distant from the preferred off-top site). This interplay between the two interaction sites is expected to play an essential role in the cluster formation on the Au(110) surface. The geometrical models for clusters are constructed by gradually adding the cysteine molecule to the sites that allow them to interact through the COOH groups, as previously pointed out in the literature.[20]

We relax the atomic positions in the adsorbed clusters in two steps: in the early stages of the structural relaxation we use a simulated annealing procedure to avoid the convergence toward a local minima of the potential energy surface. Initial temperature was set to 500 K, while the final one was set to 50 K. In the second step, the resulting structures were relaxed by using a Broyden algorithm up to a maximum gradient per atom of 0.02 eV/Å. For both stages of structural relaxation, the cysteine molecules and the two top layers of gold atoms were allowed to relax their positions, while the rest of the gold atoms were pinned to their bulk positions.

RESULTS AND DISCUSSION

Geometric Properties. The relaxed structures for periodical systems are presented in Figure 2. We chose the graphical

dx.doi.org/10.1021/jp4072857 | J. Phys. Chem. C 2013, 117, 20351−20360

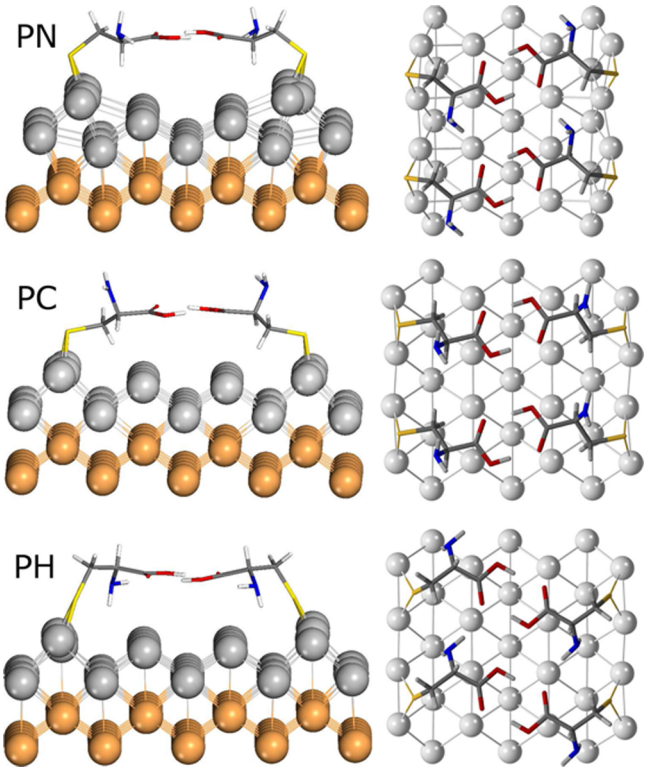

Figure 2. Graphical representation (side view, left; top view, right) of the adsorbed structures (unprotonated periodical model). We use yellow to represent deep layers and light gray for the top layers.

representation for periodic structure since in this case the surface deformation is the most important among the systems under investigation (see the discussion below). The average distances between each of the O, N, and S atoms and the surface, along the Z coordinate (i.e., perpendicular to the surface), are summarized in Table 1. As a reference for the Z coordinate we used the value of 0.5 Å (i.e., the average Z-coordinate of the atoms in the top layer of the free surface, after the relaxation). The data in Table 1 can be connected to the STM experiments, where the scan of the adsorbate gives information on the height of the adsorbed structures with respect to the surface. In particular we note that the oxygen in the COOH groups is located around 3.5 Å with relatively little variations between all models and conformers investigated. Precisely, for the PN conformers we see the extreme values, i.e., 3.36 Å, for the dimer in the protonated form, versus 4.13 Å for the periodic structure, unprotonated form. On the other hand, the PC displays the most uniform distribution of the oxygen surface, with respect to the geometrical model used in calculation. For the nitrogen atom we note differences of about 1 Å between the three conformers: in the PN structures the average distance to the surface is around 4 Å (both protonated and unprotonated forms) with a maximum of 4.4 Å for the 4PN structure. In the case of PC the average distance is around 4.7−4.8 Å (unprotonated versus protonated forms). Finally, the PH conformer allows the smallest distance between the nitrogen and gold surface; in this case the average is around 3−3.2 Å (unprotonated versus protonated forms). Sulfur position with respect to the surface is an indication of the gold−surface interaction as well as of the surface relaxation (we recall that we define the Z-coordinates in Table 1 with respect to the average position of the gold atoms in the relaxed free surface). For PC we note important modifications of the sulfur position between the dimers and periodic calculations. Precisely, the position of the S atom in the relaxed periodic structure is about 0.5 Å higher than in the adsorbed dimers. The effect is less important for PC, where the differences are smaller than 0.2 Å. Finally, for PH the values are comparable with those for PC. These findings can be easily correlated with Figure 2 where it can be seen that the adsorption of PN conformers leads to a strong deformation of the gold surface.

Precisely, in the case of periodic unprotonated PN we found that some of the gold atoms forming the rows on the Au(110) surface are pulled out from their positions in the relaxed surface. The effect is present in the case of isolated clusters, although it is weak. In the case of periodic structure, the effect is strong enough to lead to formation of an entire row of gold atoms that are displaced from their positions in the relaxed surface. To quantify the effect of surface deformation we compute the average as well as the maximum deformation induced in the surface by cysteine. We use the displacements of each atom from its equilibrium position in the relaxed isolated surface. The average deformation is defined as: $\delta x_i = x_i^0 = x_i^r$, i = 1, 2, 3, where the index i runs over the three Cartesian coordinates. The results for periodic structures (i.e., where the deformation is most important) are summarized in Table 2 together with the maximum forces acting on atoms in the surface deformed by the adsorbate. This late quantity was computed by removing the adsorbate (i.e., the cysteine molecules) from the geometric structure followed by the relaxation of the DFT wave function for the resulting systems.

For PN we note that the average displacement is oriented parallel with the O Z axis (i.e., perpendicular to the surface). The mean square errors are the most important in this case, indicating that the displacements of the gold atoms are not uniformly distributed in the surface. On the other hand, the forces acting on the gold atoms in their new positions are

Table 1. Average Distances from the S, N, and O Atoms and the Au(110) Surface for PN, PC, and PH Conformers Adsorbed on the Surface[s]

isomer	PN	PN	PN	PC	PC	PC	PH	PH	PH
model	n = 2	n = 4	$\mathcal{P}$	n = 2	n = 4	$\mathcal{P}$	n = 2	n = 4	$\mathcal{P}$
D_N [Å]	3.94	4.40	3.82	4.81	4.80	4.90	3.15	3.16	3.45
D_O [Å]	3.36	3.54	3.75	3.75	3.69	3.69	3.84	3.91	3.74
D_S [Å]	2.64	2.54	3.08	2.78	2.80	2.85	2.84	3.02	3.04
D_N^* [Å]	3.72	3.80	4.33	4.58	4.69	4.73	2.90	3.06	2.96
D_O^* [Å]	3.43	3.82	4.13	3.44	3.51	3.59	3.35	3.41	3.41
D_S^* [Å]	2.66	2.91	3.17	2.25	2.37	2.44	2.24	2.67	2.28

[s]We use the $\mathcal{P}$ symbol to designate the periodic model. Unprotonated systems are symbolized by the star symbol (*).

dx.doi.org/10.1021/jp4072857 | J. Phys. Chem. C 2013, 117, 20351−20360

Table 2. Average (δx_a, δy_a, δz_a in Å) and Maximum (δx_m, δy_m, δz_m in Å) Deformation Induced by the Adsorption on the Au(110) Surface Together with the Maximum Forces (F_i, in eV/Å) on Gold Atoms in the Periodic Systems[a]

	δx_a	δy_a	δz_a	δx_m	δy_m	δz_m	F_x	F_y	F_z
PN	0.01(0.04)	0 (0.14)	0.09(0.10)	0.01	0.12	0.11	0.07	−0.11	0.13
PC	0 (0.02)	0 (0.01)	0 (0.02)	0.03	0.04	0.05	0.24	0.05	0.28
PH	0.01 (0)	0.01 (0.01)	0.01 (0.01)	0.01	0.02	0	0.06	−0.04	0.02
PN*	0 (0.02)	0.054 (0.17)	0.11 (0.18)	0.03	0.34	0.44	0.60	−0.11	0.03
PC*	0.02(0.01)	0.01 (0.03)	0.02(0.06)	0.01	0.07	0.05	−0.55	−0.24	−0.10
PH*	0.01 (0.02)	0.02(0.02)	0.02 (0.07)	0	0.07	0.15	−0.57	−0.11	−0.46

[a]For the average values we indicate the mean square error in parentheses. Unprotonated systems are symbolized by the star symbol (*).

comparable to or even smaller than those present for PC and PH structures. This indicates that the displacements are important enough for gold atoms to reach new local energy minima on the potential energy surface. Therefore, while the system total energy is increased, the forces on the surfaces are comparable with those obtained for PC and PH. For PC and PH clusters the average displacements are smaller, with no preference for the O Z axis. In these cases the forces on gold atoms are relatively important (the exception is the PH protonated system). The conclusion is that the gold atoms are slightly displaced from their position in the relaxed surface, which leads to important energy gradients; nevertheless, it can be expected that the variation of the total energy induced by surface deformation is small in these cases, since no minimum of the potential energy is reached. In the case of unprotonated systems we note that the largest component of the gradient is oriented along the OX axis (i.e., $[1\bar{1}0]$ direction). This is a direct consequence of the double coordination of sulfur to two gold atoms (see Figure 2). Remarkably, while the sulfur is located above the gold atoms, the component of the forces on O Z direction is small in these cases.

To rationalize our findings for the adsorption of unprotonated PN, where we found a strong deformation of gold surface, we recall that Krüger et al.,[38] by using Car−Parrinello molecular dynamics simulations, demonstrate that pulling a single thiolate anchored on a stepped gold surface does not preferentially break the sulfur−gold chemical bond. Instead, it was found that the process leads to the formation of a monatomic gold nanowire, followed by breaking a gold−gold bond with a rupture force of about 1.2 nN. Their study was focused on the rupture process of an ethylthiolate molecule (CH_3−CH_2−S) on gold at room temperature. In the case of PN clusters we point out that the presence of a strong deformation of the gold surface is due to the interaction between the sulfur and two gold atoms coordinated to it. As a result, the gold atoms are displaced from their ideal position, as indicated above. Ultimately, the result is the displacement of a whole chain of atoms on the Au(110) surface. This proves that the formation of the periodic unprotonated chains is capable of a surface reconstruction, similar to the results found by Kühnle et al.[21] In addition to the experimental findings, we can argue that the surface reconstruction is the most probable in the case of PN clusters.

Binding Energy. Let us now investigate the potential energy surface of the adsorbate with respect to the bending angle θ as defined in the inset of Figure 3. Precisely after the full relaxation of the adsorbate we rotate each molecule around the $[1\bar{1}0]$ axis in opposite directions, by keeping the sulfur atoms fixed. Figure 3 shows the value of the difference $E_\theta - E_0$ between total energy of metal−adsorbate structure for different rotation angles, E_θ, and the energy of the relaxed systems, E_0,

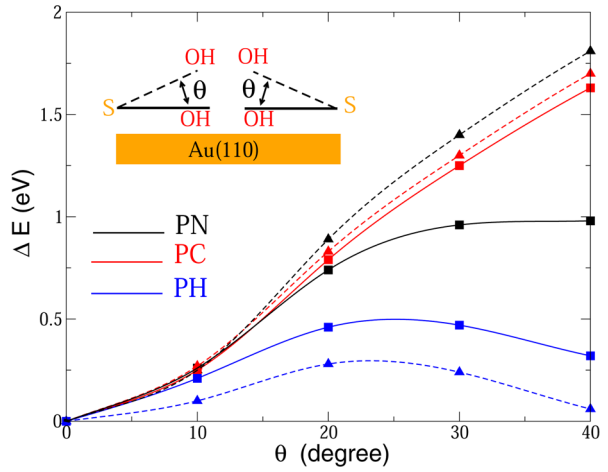

Figure 3. Dependence of the $E_\theta - E_0$ energy difference on the rotation angle θ defined in the inset, for the unprotonated cysteine clusters on the Au(110) surface. Line: dimers on the surface; dashed line: periodic structure. The rotation is performed on the axis parallel with the $[1\bar{1}0]$ direction that contains the S atom.

for each of the three types of dimers as well as for periodic structures (unprotonated systems). We choose to perform this study only for unprotonated systems to get rid of the spurious contributions resulting from the interaction of the hydrogen in the S−H group and the gold surface.

For PN we notice that the height of the energy barrier separating the relaxed structure and the configuration with the molecules oriented at 45° with respect to the plane of the Au(110) surface is close to the computational accuracy for isolated dimers, while for periodic structure there is no energy barrier between the two geometric configurations. It can be seen that for the PC form there is no energy barrier between the two configurations. Finally, for the PH conformer we notice the most important barrier between the two configurations (i.e., about 0.14 eV for dimers and 0.2 eV for periodic structure).

While these results do not fully describe the potential energy surface leading to formation of molecular rows on Au(110), by rotation around the $[1\bar{1}0]$ axis, they indicate that we can expect important differences between the dynamics of dimer formation from two units adsorbed on parallel rows on the Au(110) surface. Such differences are clearly dependent on the type of rotational conformer used in the geometric model. Let us note that we can correlate the results from Figure 3 with the distance between nitrogen and the gold surface. Precisely, the largest distance (i.e., PC conformers) leads to a potential energy surface with no barrier. On the other hand, for PH the situation is the opposite: the smallest distance between nitrogen and the gold surface leads to the most important energy barrier in Figure 3. Finally, the intermediate case (i.e., PN) leads to

dx.doi.org/10.1021/jp4072857 | J. Phys. Chem. C 2013, 117, 20351−20360

intermediate values for the energy barrier. We think this is a direct consequence of the fact that the NH_2 group is located outside of the ideal position it prefers in the case of single molecule adsorption (i.e., on the off-top of gold atoms[27]).

On the other hand, the results in Figure 3 indicate that for the PN conformer the rotational energy barrier dramatically changes in the presence of periodic boundary conditions. We recall the experimental result from ref 20 where it was found that the formation of new nucleation centers is more difficult compared to the continuation of an existing row.[20] While our periodic calculation does not provide a model for the attachment of a new pair of cysteine units to the already formed row, it indicates that the presence of other additional cysteine units on the surface can reduce the energy barrier indicated in Figure 3. We conclude that this result is in qualitative agreement with the experimental results.[20] Also, Figure 3 clearly shows that such an effect occurs only for the PN conformer, while for PC or PH no significant changes of the potential energy surface are present if we go from an isolated cluster to a periodic boundary conditions model (i.e., long, infinite rows adsorbed on the surface).

We continue our investigation by analyzing the binding energies of the adsorbates. First we note that according to our calculations the most stable (i.e., the lowest total DFT energy) among the three conformers is the PH; the PN has a total energy 0.03 eV higher, while for the PC the total energy is 0.25 eV higher. According to these values at room temperature (i.e., about 0.027 eV) we can expect to find both PN and PC conformers.

Next we evaluate the binding energy per cysteine unit in each adsorbed structure as

$$\Delta E^{a} = \frac{\mathcal{E}_{\mathcal{T}} - [n \times E_1 + \mathcal{E}_S]}{n} \quad (1)$$

where $\mathcal{E}_{\mathcal{T}}$ is the total DFT energy for the relaxed surface−cluster system and $\mathcal{E}_S$ is the energy of the relaxed surface. The quantity E_1 is the total energy of a single relaxed cysteine unit, while n is the number of cysteine units in the cluster (i.e., 2 or 4). The BSSE corrections are included in the binding energies summarized in Figure 4.

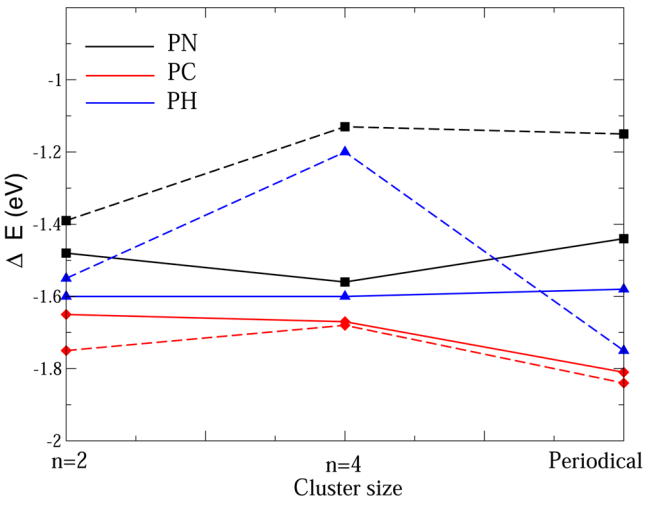

Figure 4. Binding energies for the clusters formed by PN, PC, and PH conformers adsorbed on Au(110), protonated form (line) and unprotonated (dashed line).

For PN the binding energies of unprotonated form are smaller, compared to protonated ones. This can be partially explained by the strong surface deformation induced by the adsorption of the PN conformer, as discussed above. We also note that the formation of new nucleation centers for cysteine rows (i.e., the transition from an adsorbed dimer to two dimers, including 4 cysteine units) occurs in a different manner for protonated/unprotonated forms. Indeed, for the unprotonated form the formation of a structure with 4 cysteine units leads to an energetic destabilization with about 0.22 eV. Furthermore, the formation of long (periodic) rows leads to a small stabilization. For the protonated form the behavior is the opposite: the 4PN is stabilized with respect to 2PN, while the formation of periodic structure brings a small energetic destabilization. Overall, we can conclude that in the case of PN clusters the formation of small structures (2 or 4, depending on the protonation form) is energetically favorable, against the formation of long/periodic rows.

For the PC form a small energy barrier (about 0.12 eV) is present at the formation of the 4PC system, in unprotonated form. Next, the formation of periodic rows leads to energetic stabilization of the system for both protonated and unprotonated forms. Moreover, for the PC conformer the average differences in the binding energy of different configurations were found to be the smallest among the three conformers. We think that the lack of direct interaction between NH_2 and the surface is responsible for this behavior.

For the PH form we note a behavior of the binding energy as a function of geometrical model that is rather similar to that for PN. While for the protonated form the binding energy per cysteine unit is roughly a constant value for geometric models including dimers, double-dimers, and periodic structures, the unprotonated form leads to an important destabilization of the 4PH model. Precisely, the binding energy per dimer decreases with about 0.35 eV in the double dimer, compared to that obtained for the adsorbed dimer. Furthermore, the periodic model brings an energetic stabilization with about 0.15 eV compared to the adsorption of an isolated dimer.

Finally, we note that the results for unprotonated conformers are in agreement with the experimental finding indicating that the formation of new nucleation centers is energetically unfavorable to the continuation of the self-assembly process along an existing row.[20] Indeed, for all models investigated by us the double-dimer systems decrease their binding energy in unprotonated form, if compared with both dimers or periodic structures. In addition to that, our results suggest that this effect is rather weak in the case of the PC conformer.

Electronic Structure and Charge Transfer. To understand the electronic structure of the adsorbed clusters we focus on the analysis of the projected density of states (PDOS) and the molecule−surface charge transfer. The analysis of the PDOS for isolated molecules is presented in Figure 5. We note that all three conformers display a HOMO−LUMO gap around 3.6 eV, with a slightly reduced value in the unprotonated form. The gap between HOMO-1 and HOMO orbitals is maximized for the PN conformer (about 0.55 eV), while for PC its value is smallest (i.e., 0.3 eV). For PH an intermediate value of 0.4 eV occurs. The chemical properties of the three conformers in the protonated form are slightly different. While the HOMO of PN is dominated by a contribution from the sulfur, for PC the nitrogen is responsible for about 80% of the HOMO peak. Finally, the PH displays an intermediate structure, with equal contributions from S and N atoms in the HOMO orbital.

dx.doi.org/10.1021/jp4072857 | J. Phys. Chem. C 2013, 117, 20351−20360

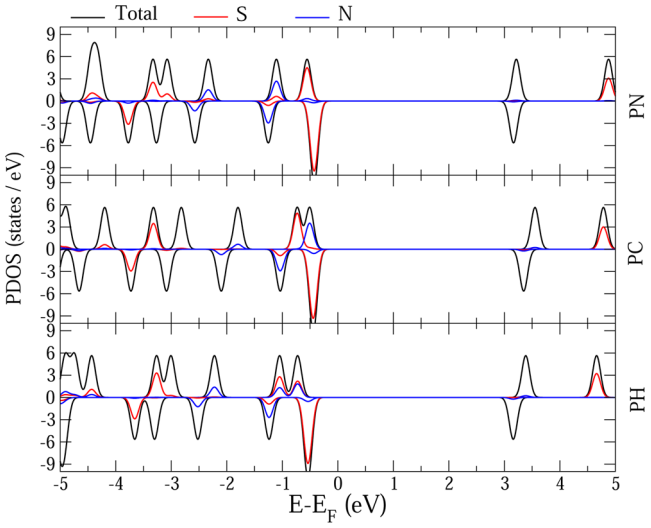

Figure 5. Total and atom-projected density of states for the cysteine conformers PN, PC, and PH. We lined up the vacuum level of (average value of the Hartree potential in vacuum) in the molecules with that of the clean relaxed Au(110) surface.

Remarkably, the LUMO does not display any contribution of the sulfur or nitrogen. In the unprotonated form, the density of states of three conformers is more homogeneous, with a dominant contribution of sulfur to the HOMO orbital.

A comparison between the PDOS of the adsorbed cysteine clusters for the three conformers is given in Figure 6, Figure 7,

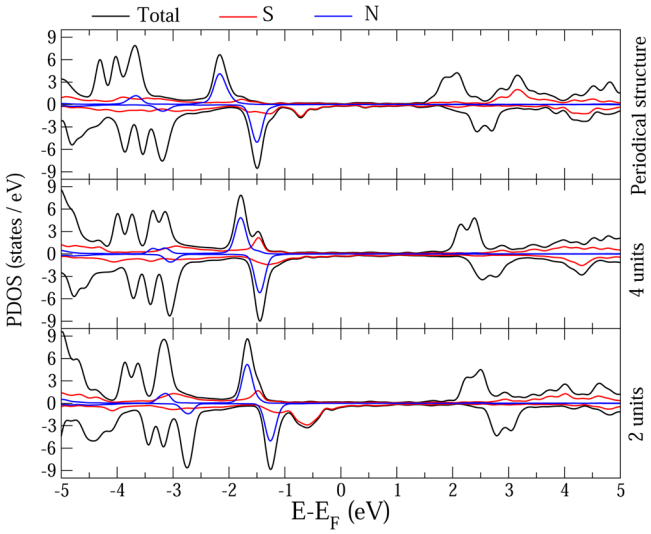

Figure 6. Total and atom-projected density of states for the cysteine clusters in the PN form adsorbed on the Au(110) surface. Top values are for the protonated structures, while the bottom ones are for unprotonated structures.

and Figure 8, respectively. Please note that to compare directly the results for the three geometric models we divide by two the PDOS for double dimers (i.e., we normalize the results to a geometric structure including two cysteine units.)

As a general comment let us observe the presence of an overall shift of DOS as a function of number of units included in the model (2, 4, or periodic model). This effect was already pointed out by our previous study on the adsorption of cysteine clusters[39] and indicates an energetic stabilization trend. This

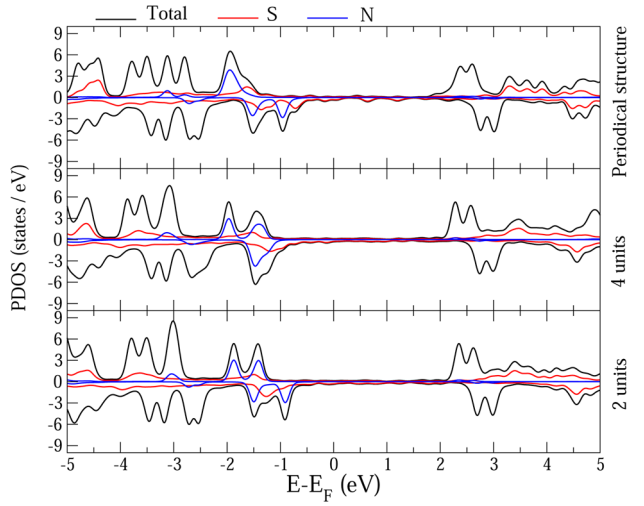

Figure 7. Total and atom-projected density of states for the cysteine clusters in the PC form adsorbed on the Au(110) surface. Top values are for the protonated structures, while the bottom ones are for unprotonated structures.

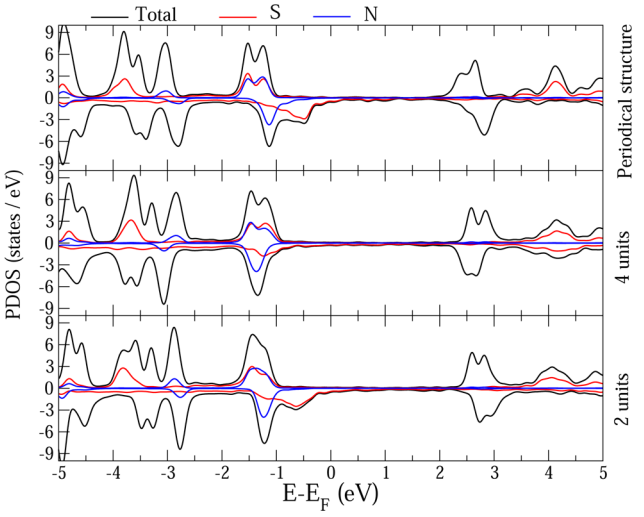

Figure 8. Total and atom-projected density of states for the cysteine clusters in the PH form adsorbed on the Au(110) surface. Top values are for the protonated structures, while the bottom ones are for unprotonated structures.

can be explained by the increased number of quantum states available in complex clusters, compared to the states available to isolated units. We note that the effect is not present in the PH clusters. Let us now discuss in detail the specific features for each conformer.

For PN we note that the HOMO and HOMO-1 of the adsorbed molecule display the sharpest peaks among all systems. This is probably caused by the gap between the HOMO and HOMO-1 orbital present in the free conformer. In particular, the peaks of nitrogen are well-defined; for the protonated form they are located around −1.6 to −2.2 eV below the Fermi level. As expected, the sulfur peak is broadened and depleted with respect to the isolated molecule. For the protonated form, it is located around −1.4 eV. We note that in the periodic structure the depletion is even stronger, and the peak is shifted toward −1.9 eV. In the unprotonated form we note that the sulfur peak for the dimer structure is close to −0.6 eV; remarkably, in the double dimer structure this peak is

dx.doi.org/10.1021/jp4072857 | J. Phys. Chem. C 2013, 117, 20351−20360

Table 3. Integral Over the $\Delta\rho(\vec{r})$ for the Clusters Formed by PN, PC, and PH Conformers Adsorbed on Au(110) for Protonated (Q) and Unprotonated (Q^*) Structures[a]

isomer	PN	PN	PN	PC	PC	PC	PH	PH	PH
model	$n = 2$	$n = 4$	$\mathcal{P}$	$n = 2$	$n = 4$	$\mathcal{P}$	$n = 2$	$n = 4$	$\mathcal{P}$
Q ($\|e\|$)	0.18	0.27	0.18	0.21	0.38	0.14	0.04	0.07	0.04
Q^* ($\|e\|$)	−0.05	0.02	0.01	0.04	0.14	0.05	−0.05	0.15	−0.05

[a]For the clusters with $n = 4$ molecules we divide the results by a factor of two in order to get a direct comparison with the values obtained for geometric models with two cysteine units.

strongly depleted, while in the periodic structure it appears around −0.7 eV. This indicates that the formation of nucleation centers occurs with a perturbation of the electronic structure of the S−Au bond.

In the case of PC, where the nitrogen is located at the largest distance with respect to the surface, the nitrogen peaks are splitted and depleted. Also, as a general trend, the peaks of PDOS are broader if compared to those obtained for PN. We think that the small gap between HOMO and HOMO-1 in the isolated molecule is responsible for this behavior since the tunnelling between the metal and molecular states is facilitated. For isolated clusters in the protonated forms, the nitrogen peak is located around −1.5 eV below the Fermi level; in these cases a second nitrogen peak is present around −2 eV. In the periodic structure, only this second peak appears around −2 eV. The sulfur peaks are strongly depleted and are localized slightly below −1.5 eV for all structures. For unprotonated forms we notice also the presence of two peaks for the nitrogen. Again, the double dimer is different compared to the isolated dimer and periodic structure. Precisely, in these late two structures a gap of about 0.5 eV between the two peaks is present, while for the double dimer this gap is reduced to less than a half. The sulfur contribution is located around −1.2 eV. In the periodic structure it splits into two peaks around −0.7 and −1.4 eV.

Finally, for the PH conformer the protonated structures display the broadest nitrogen peaks. In the dimer structure a large peak is present around −1.5 eV, while for the other two structures two peaks are present, around −1.3 and −1.5 eV. Remarkably, the nitrogen and sulfur peaks are almost overlapped in this case, suggesting the presence of a chemical interaction between the two atoms. In the unprotonated form, all three structures display a nitrogen peak around −1.3 eV, while the interaction with sulfur is not present. We also remark that the sulfur has a peak close to −0.6 eV in the dimer structure and −0.5 eV, respectively, in the periodic one. For the double dimer this peak is strongly depleted and located around −1.2 eV. In this case we can say that the formation of nucleation centers leads to a modification of the electronic structure of the S−Au bond.

Let us now investigate the spatially resolved charge-density difference, defined as

$$\Delta\rho(\vec{r}) = \rho_{\mathcal{T}}(\vec{r}) - [\rho_{\mathcal{C}}(\vec{r}) + \rho_{\mathcal{S}}(\vec{r})] \quad (2)$$

where $\rho_{\mathcal{T}}(\vec{r})$, $\rho_{\mathcal{C}}(\vec{r})$, and $\rho_{\mathcal{S}}(\vec{r})$ are the (negative) charge densities of the relaxed adsorbate−substrate system (total system $\mathcal{T}$), adsorbate without substrate (cluster, $\mathcal{C}$), and clean surface ($\mathcal{S}$), respectively .

By starting from eq 2 we estimate the molecule−surface charge transfer and the formation of the interface dipoles. These can be computed by integrating $\Delta\rho(\vec{r})$ over selected spatial domains on the surface. Precisely, we divide the ad-structure into two regions by a plane parallel to the metal's surface. The former one contains the ad-molecule, and the latter one contains the surface.[40] We define the two regions by choosing a plane parallel to the metal surface and located at 1.35 Å (protonated) and 1.25 Å (unprotonated) distance from it (i.e., close to the plane that bisects the ad-system at the vertical position). The results for all systems are summarized in Table 3. While these results obviously depend on the position of the bisection plane, they can still provide valuable information for the surface dipole formation. By choosing a given separation plane between the molecule and surface and by computing the charge transfer defined by it, we get a reasonable hint for the value of the surface dipole. We note that the electric charge on the molecule is positive for all protonated systems (i.e., the electrons migrate from the molecule to the surface). The same is valid for the majority of uprotonated systems but with smaller values; the exceptions are PN and PH dimers, where small negative charge occurs. To check the robustness of our results, we performed all calculations for a separation plane molecule−surface located at 0.9 Å above the surface. We found a good qualitative agreement between the results. The most important differences occur for the unprotonated 4PH system (0.03 $|e|$ versus 0.15 $|e|$).

The integration of $\Delta\rho(\vec{r})$ over the adsorbate region gives larger values for the protonated systems, compared with those for the unprotonated ones. We think that this is an indication that in the case of protonated systems the physisorption (therefore the interface dipole) plays the dominant role in the adsorption, while for the unprotonated systems the chemical bond between the sulfur and gold dominates the molecule−metal structures.

A second type of information to be extracted from eq 2 is related to the formation of the S−Au bond. Precisely, the charge fluctuations induced by the surface are an indication of the bond formation between sulfur and gold. A graphical representation of $\Delta\rho(\vec{r})$ along the shortest S−Au bond in the adsorbed dimers is given in Figure 9. By inspecting Figure 9 we first note the differences between protonated and unprotonated systems. Precisely, in the case of unprotonated systems, the charge fluctuation in the vicinity of gold atoms is about four times more important than the same quantity in the protonated systems. Also, we note that the sulfur−gold distances have average values of about 2.8 Å (protonated systems) and 2.5 Å for unprotonated ones. Remarkably, for protonated PH the sulfur−gold distance is 3.6 Å (i.e., about 40% larger compared to the average value of 2.5 Å obtained for PN and PC). This important increase of the sulfur−gold distance does not reflect a similar variation of the binding energy of the adsorbate. Consequently, we expect the interaction mechanism between the molecule and surface to be different with respect to that occurring for PN and PC. We think that the orientation of the NH_2 group toward the surface is responsible for this behavior. In the case of unprotonated systems the S−Au interaction is sufficiently strong to suppress the physical repulsion between

dx.doi.org/10.1021/jp4072857 | J. Phys. Chem. C 2013, 117, 20351−20360

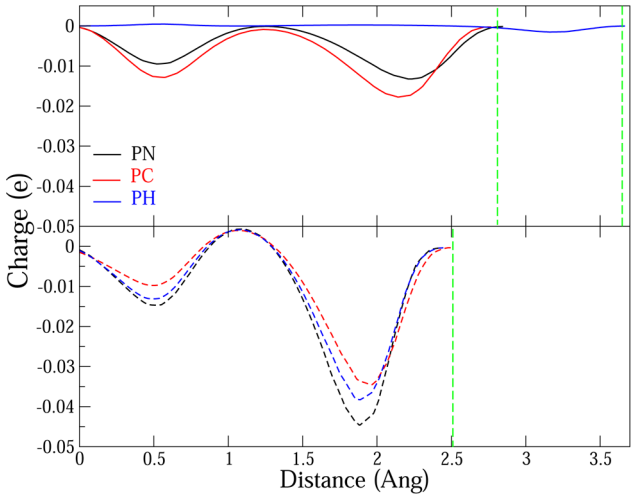

Figure 9. Values of $\Delta\rho(\vec{r})$ along the S−Au bond in the adsorbed dimers. Top: protonated systems; bottom: unprotonated systems. The origin of the plot is on the S atom. Green lines indicate approximatively the position of the gold atom relative to the S.

NH_2 and the surface, leading to a S−Au distance that is similar for PN, PC, and PH.

Alternatively, the analysis of metal−adsorbate charge transfer can be performed in terms of Voronoi and/or Hirschfeld atomic charges.[41,42] The sums over Voronoi and Hirschfeld charges over atoms in the adsorbed structures are listed in Table 4. By inspecting the values we see that for protonated systems the total electric charge is positive in the case of PN and PC, while for PH they are negative. These results are slightly different from those presented in Table 3. The difference between the two is probably an indication of the fact that a depletion of the electronic density in the regions between atoms takes place; this emphasizes the role of interface dipole for the metal−adsorbate interaction, in the case of protonated systems. The formation of nucleation centers (i.e., differences between geometric models including 2 and 4 molecules and periodic models) does lead to variations of the electronic population per dimer that are less than 0.08 |e|. The same is the case for the formation of molecular rows that leads to variations of less than 0.1 |e| for the electronic populations.

For all unprotonated systems, the electric charges are negative and relatively important. Again, by comparing these results with those listed in Table 3 we note relatively important differences, indicating the reorganization of electric density over the whole adsorbate. For PN we note an important fluctuation of electronic population brought by the formation of rows on the surface: the total population per dimer is around −0.45 |e|, while the same quantity drops to about −0.25 |e| in 4PN and periodic structure. For PC we see no dependence of the charge transfer on the geometric configuration; this is probably an indication of the fact that the interaction S−Au is dominant in comparison with the interaction between cysteine molecules in the row. In the case of PH clusters the effect of the NH_2 group is visible in the value of the total charge transfer—which displays the largest values among the three models.

We notice important differences of total atomic populations at the formation of new nucleation centers for PN and PH systems. Indeed, the difference between the electric charges per dimer between 2PN and 4PN systems is around 0.18 |e|, while the PH displays a value of 0.21 |e|. We note that these results are in agreement with our previous findings based on the analysis of the total binding energy. For PC on the other hand we find no significant changes between the 2 and 4 molecule structures.

We note that the electric charge of the nitrogen atom is almost constant, regardless of the geometrical model used. The variations are from −0.19 |e| obtained for 4PC and 4PN systems to −0.21 |e|, obtained for 2PH* and 4PH* adsorbates. The same is valid for the oxygens, where the electronic population is in all cases around −0.2 |e|. This strong electronegative character will force electrons in other regions of the molecule (especially of the hydrogen) to reorganize to interact with the surface. Nevertheless, these values are rather small and range for periodic structures from 0.05 |e| for PH to 0.1 |e| in the case of the PC system.

CONCLUSION

We have studied the formation of the cysteine clusters on the relaxed Au(110)-(1 × 1) surface by means of density-functional-theory calculations within the framework of LCAO and norm-conserving pseudopotentials. The total energy optimizations with respect to the atomic positions have been accompanied by investigations of the electron transfer and the changes in the electronic structure of molecule and substrate upon adsorption. The studies were focused on the comparison of the adsorption mechanisms for clusters formed by three rotational conformers of cysteine (i.e., PN, PC, and PH conformers). For each conformer we investigated geometric models relevant for the formation of new nucleation centers on the surface (i.e., isolated clusters), as well as periodic models, describing the long rows of adsorbate attached to the surface.

As already pointed out, the adsorption of a single cysteine molecule favors a flat configuration with a sulfur atom at an off-bridge site and NH_2 group at an off-top site. When the clusters of different conformers are formed by starting with an off-bridge position of the S atoms, the interaction of the NH_2 with the surface leads to a rather complex behavior. Precisely, in the case of PN conformer the NH_2 group is located at about 4 Å to

Table 4. Sum of the Hirschfeld and Voronoi Charges Over the Atoms in the Clusters Formed by PN, PC, and PH Conformers Adsorbed on Au(110), Protonated Form (N_H and N_V), and Unprotonated (N_H^* ans N_V^*) Structures[a]

isomer	PN	PN	PN	PC	PC	PC	PH	PH	PH
model	$n = 2$	$n = 4$	$\mathcal{P}$	$n = 2$	$n = 4$	$\mathcal{P}$	$n = 2$	$n = 4$	$\mathcal{P}$
N_H (|e|)	0.04	0.01	0.09	0.15	0.07	−0.03	−0.14	−0.15	−0.07
N_H^* (|e|)	−0.45	−0.27	−0.26	−0.28	−0.29	−0.31	−0.47	−0.28	−0.42
N_V [|e|]	0.07	0.03	0.13	0.19	0.11	0.01	−0.10	−0.11	−0.05
N_V^* [|e|]	−0.42	−0.24	−0.24	−0.25	−0.26	−0.27	−0.47	−0.26	−0.42

[a]For the clusters with $n = 4$ molecules we divide the results by a factor of two to get a direct comparison with the values obtained for geometric models with two cysteine units.

dx.doi.org/10.1021/jp4072857 | J. Phys. Chem. C 2013, 117, 20351−20360

the surface, in a position that allows it to interact with the neighbors in the rows formed on the surface. In this case we found that a strong deformation of the surface occurs in the case of adsorption of unprotonated periodic structures. We point out the presence of an energy barrier at the formation of new nucleation centers, in special for unprotonated systems. In the case of the PC conformer we found the most stable structures as well as the most convenient shape of the potential energy surface. Remarkably, in the PC conformers the NH_2 group is located at a high position relative to the surface (i.e., about 5 Å) which reduces significantly its interaction with the surface. The formation of nucleation centers as well as the formation of rows along the $[1\bar{1}0]$ direction are favored if the PC conformer of cysteine is used. Finally in the PH conformers the NH_2 group lies at about 3 Å to the surface; this allows it to directly interact with the gold surface. In this case we found one of the lowest binding energies per molecule and a structure of the potential energy surface which is unfavorable for the formation of rows.

Our results should be relevant for the understanding of physicochemical properties of self-assembled cysteine monolayers and other higher coverage structures. Also, we think our study provides useful information for fabrication of the cysteine rows assembled on Au(110) surfaces.

AUTHOR INFORMATION

Corresponding Author

*E-mail: cristian.morari@itim-cj.ro. Phone: +40 264 584037. Fax: +40 264 420042.

Notes

The authors declare no competing financial interest.

ACKNOWLEDGMENTS

Financial support from the Romanian UEFISCDI is acknowledged (Project No.1/31.05.2012, PN-II-ID-PCCE-2011-2-0027). All the calculations were performed at the Data Center of NIRDIMT, Cluj-Napoca.

REFERENCES

(1) Smith, R. K.; Lewis, P. A.; Weiss, P. S. Patterning Self-Assembled Monolayers. *Prog. Surf. Sci.* **2004**, *75*, 1−68.
(2) Love, J. C.; Estroff, L. A.; Kriebel, J. K.; Nuzzo, R. G.; Whitesides, G. M. Self-Assembled Monolayers of Thiolates on Metals as a Form of Nanotechnology. *Chem. Rev.* **2005**, *105*, 1103−1169.
(3) Whitesides, G. M.; Kriebel, J. K.; Love, J. C. Molecular Engineering of Surfaces Using Self-Assembled Monolayers. *Sci. Prog.* **2005**, *88*, 17−48.
(4) Ulman, A., Ed., Self-Assembled Monolayers of Thiols. *Thin Films*; Academic Press: San Diego, 1998; Vol. *24*.
(5) Nilsson, A.; Pettersson, L. G. M. Chemical Bonding on Surfaces Probed by X-ray Emission Spectroscopy and Density Functional Theory. *Surf. Sci. Rep.* **2004**, *55*, 49−167.
(6) Ishii, H.; Sugiyama, K.; Eisuke, I.; Seki, K. Energy Level Alignment and Interfacial Electronic Structures at Organic/Metal and Organic/Organic Interfaces. *Adv. Mater. (Weinheim, Ger.)* **1999**, *11*, 605−625.
(7) Heimel, G.; Romaner, L.; Brédas, J.-L.; Zojer, E. Band Lineup and Interface Energetics at Covalent Metal-Molecule Junctions: π-Conjugated Thiols on Gold. *Phys. Rev. Lett.* **2006**, *96*, 196806.
(8) De Renzi, V.; Rousseau, R.; Marchetto, D.; Biagi, R.; Scandolo, S.; del Pennino, U. Metal Work-Function Changes Induced by Organic Adsorbates: a Combined Experimental and Theoretical Study. *Phys. Rev. Lett.* **2005**, *95*, 046804.
(9) Rauls, E.; Blankenburg, S.; Schmidt, W. G. DFT Calculations of Adenine Adsorption on Coin Metal (110) Surfaces. *Surf. Sci.* **2008**, *602*, 2170−2176.
(10) Bilić, A.; Reimer, J. R.; Hush, N. S.; Hafner, J. Accurate Computational Methods for Gold Ligand Complexes: Application to $AuNH_3$. *Chem. Phys.* **2002**, *116*, 10277−10286.
(11) Morari, C.; Rignanese, G. M.; Melinte, S. Electronic Properties of 1−4,dicyanobenze and 1−4,diisocyanidebenzen Molecules Contacted Between Two Platinum and Palladium Electrodes: A First-Principles Study. *Phys. Rev. B* **2007**, *76*, 115428.
(12) Xue, Y.; Datta, S.; Ratner, M. A. Charge Transfer and Band Lineup in Molecular Electronic Devices: A Chemical and Numerical Interpretation. *J. Chem. Phys.* **2001**, *115*, 4292−4300.
(13) Tonigold, K.; Gross, A. Adsorption of Small Aromatic Molecules on the (111) Surfaces of Noble Metals: A Density Functional Theory Study with Semiempirical Corrections for Dispersion Effects. *J. Chem. Phys.* **2010**, *132*, 224701−224711.
(14) Kühnle, A.; Linderoth, T. R.; Besenbacher, F. Enantiospecific Adsorption of Cysteine at Chiral Kink Sites on Au(110)-(1 × 2). *J. Am. Chem. Soc.* **2006**, *128*, 1076−1077.
(15) Kühnle, A.; Linderoth, T. R.; Schunack, M.; Besenbacher, F. L-Cysteine Adsorption Structures on Au(111) Investigated by Scanning Tunneling Microscopy Under Ultra-High Vacuum Conditions. *Langmuir* **2006**, *22*, 2156−2160.
(16) Mirkin, C. A; Letsinger, R. L.; Mucic, R. C.; Storhoff, J. J. A DNA-Based Method for Rationally Assembling Nanoparticles into Macroscopic Materials. *Nature (London)* **1996**, *382*, 607−609.
(17) Plekan, O.; Feyer, V.; Ptasińska, S.; Tsud, N.; Cháb, V.; Matolín, V.; Prince, K. C. Photoemission Study of Thymidine Adsorbed on Au(111) and Cu(110). *J. Phys. Chem. C* **2010**, *114*, 15036−15041.
(18) Feyer, V.; Plekan, O.; Prince, K. C.; Šutara, F.; Skála, T.; Cháb, V.; Matolín, V.; Stenuit, G.; Umari, P. Bonding at the organic/metal interface: Adenine to Cu(110). *Phys. Rev. B* **2009**, *79*, 155432.
(19) Kühnle, A.; Linderoth, T. R.; Hammer, B.; Besenbacher, F. Chiral Recognition in Dimerization of Adsorbed Cysteine Observed by Scanning Tunnelling Microscopy. *Nature (London)* **2002**, *415*, 891−893.
(20) Kühnle, A.; Molina, L. M.; Linderoth, T. R.; Hammer, B.; Besenbacher, F. Growth of Unidirectional Molecular Rows of Cysteine on Au(110)-(1 × 2) Driven by Adsorbate-Induced Surface Rearrangements. *Phys. Rev. Lett.* **2004**, *93*, 086101.
(21) Kühnle, A.; Linderoth, T. R.; Besenbacher, F. Self-Assembly of Monodispersed, Chiral Nanoclusters of Cysteine on the Au(110)-(1 × 2) Surface. *J. Am. Chem. Soc.* **2003**, *125*, 14680−14681.
(22) Greber, T.; Šljivančanin, Ž.; Schillinger, R.; Wider, J.; Hammer, B. Chiral Recognition of Organic Molecules by Atomic Kinks on Surfaces. *Phys. Rev. Lett.* **2006**, *96*, 056103.
(23) Schillinger, R.; Šljivančanin, Ž.; Hammer, B.; Greber, T. Probing Enantioselectivity with X-Ray Photoelectron Spectroscopy and Density Functional Theory. *Phys. Rev. Lett.* **2007**, *98*, 136102.
(24) Šljivančanin, Ž.; Gothelf, K.; Hammer, B. Density Functional Theory Study of Enantiospecific Adsorption at Chiral Surfaces. *J. Am. Chem. Soc.* **2002**, *124*, 14789−14794.
(25) Di Felice, R.; Selloni, A.; Molinari, E. DFT Study of Cysteine Adsorption on Au(111). *J. Phys. Chem. B* **2003**, *107*, 1151−1156.
(26) Di Felice, R.; Selloni, A. Adsorption modes of cysteine on Au(111): thiolate, amino-thiolate, disulfide. *J. Chem. Phys.* **2004**, *120*, 4906−4914.
(27) Höffling, B.; Ortmann, F.; Hannewald, K.; Bechstedt, F. Single Cysteine Adsorption on Au(110): A First-Principles Study. *Phys. Rev. B* **2010**, *81*, 045407.
(28) Buimaga-Iarinca, L.; Calborean, A. Electronic Structure of the ll-Cysteine Dimers Adsorbed on Au(111): A Density Functional Theory Study. *Phys. Scr.* **2012**, *86*, 035707.
(29) Wilke, J. J.; Lind, M. C.; Schaefer, H. F., III; Csaszar, A. G.; Allen, W. D. Conformers of Gaseous Cysteine. *J. Chem. Theory Comput.* **2009**, *5*, 1511−1523.

(30) Graff, M.; Bukowska, J. Adsorption of Enantiomeric and Racemic Cysteine on a Silver Electrode - SERS Sensitivity to Chirality of Adsorbed Molecules. *J. Phys. Chem. B* **2005**, *109*, 9567−9574.
(31) Ordejón, P.; Artacho, E.; Soler, J. M. Self-Consistent Order-N Density-Functional Calculations for Very Large Systems. *Phys. Rev. B* **1996**, *53*, R10441−R10444.
(32) Soler, J. M.; Artacho, E.; Gale, J. D.; García, A.; Junquera, J.; Ordejón, P.; Sánchez-Portal, D. The Siesta Method for Ab Initio Order-N Materials Simulation. *J. Phys.: Condens. Matter* **2002**, *14*, 2745−2779.
(33) Troullier, N.; Martins, J. L. Structural and Electronic Properties of C_{60}. *Phys. Rev. B* **1992**, *46*, 1754−1765.
(34) Sankey, O. F.; Niklewski, D. J. Ab-initio Multicenter Tight-binding Model for Molecular-Dynamics Simulations and Other Applications in Covalent Systems. *Phys. Rev. B* **1989**, *40*, 3979−3995.
(35) Huzinaga, S., Ed. *Gaussian Basis Sets for Molecular Calculations*; Elsevier: Berlin, 1984.
(36) Bachelet, G. B.; Hamann, D. R.; Schluter, M. Pseudopotentials That Work: From H to Pu. *Phys. Rev. B* **1982**, *26*, 4199−4228.
(37) Hammer, B.; Hansen, L. B.; Nø rskov, J. K. Improved Adsorption Energetics Within Density-Functional Theory Using Revised Perdew-Burke-Ernzerhof Functionals. *Phys. Rev. B* **1999**, *59*, 7413−7421.
(38) Krüger, D.; Fuchs, H.; Rousseau, R.; Marx, D.; Parrinello, M. Pulling Monatomic Gold Wires with Single Molecules: An Ab Initio Simulation. *Phys. Rev. Lett.* **2002**, *89*, 186402.
(39) Buimaga-Iarinca, L.; Morari, C. Adsorption of Cysteine Clusters on Au(110)-(1 × 1) Surface: A DFT Study. *RSC Adv.* **2013**, *3*, 5036−5044.
(40) Bogdan, D.; Morari, C. Electronic Properties of DNA Nucleosides Adsorbed on a Au(100) Surface. *J. Phys. Chem. C* **2012**, *116*, 7351−7359.
(41) Bickelhaupt, F. M.; van Eikema Hommes, N. J. R.; Fonseca Guerra, C.; Baerends, E. J. The Carbon - Lithium Electron Pair Bond in $(CH_3Li)_n$ (n = 1, 2, 4). *Organometallics* **1996**, *15*, 2923−2931.
(42) Hirshfeld, F. L. Bonded-Atom Fragments for Describing Molecular Charge Densities. *Theor. Chim. Acta* **1977**, *44*, 129−138.